ISSN 0029-3865

CBPF-NF-023/84

QUENCHED RANDOM-BOND ISING FERROMAGNET. II. ANISOTROPIC CONCENTRATIONS

by

E.F. Sarmento*, C. Tsallis**+ and R. Honmura*

+Centro Brasileiro de Pesquisas Físicas - CNPq/CBPF
Rua Dr. Xavier Sigaud, 150
22290 - Rio de Janeiro, RJ - Brazil

*Departamento de Física
Universidade Federal de Alagoas
57000 - Maceió, AL - Brazil

QUENCHED RANDOM-BOND ISING FERROMAGNET. II. ANISOTROPIC CONCENTRATIONS

E.F. Sarmento*

Constantino Tsallis*+

R. Honmura*

*Departamento de Física, Universidade Federal de Alagoas, 57000 Maceió, AL, Brazil

+Permanent address: Centro Brasileiro de Pesquisas Físicas/CNPq, Rua Dr. Xavier Sigaud, 150 22290 Rio de Janeiro, RJ, Brazil

Abstract

We have recently introduced an effective-field framework which, without mathematical complexities, enables the calculation of the phase diagram (and magnetization) associated with a quenched bond-mixed spin-$\frac{1}{2}$ Ising model in an anisotropic simple cubic lattice. The case corresponding to anisotropic coupling constants but isotropic concentrations was discussed in detail in that occasion. Herein we discuss the case corresponding to isotropic coupling constants but *anisotropic* concentrations. A certain amount of interesting phase diagrams are exhibited; whenever comparison with available data is possible, the present results provide a satisfactory qualitative (and to a certain extent quantitative) agreement.

Key-words: Ising; Random Magnetism; Anisotropic; Phase Diagrams.

PACS Index: 75.10.Hk; 75.40.Dy; 75.10.-b; 64.60.-i.

I. INTRODUCTION

Random magnetism has been intensively focused during last years, both theoretically and experimentally (see Ref. 1 and references therein). Two of us have recently presented, in a paper[1] hereafter referred to as paper I, an effective-field theoretical framework which enables the discussion of a quite general Ising model. To be more specific the model is the quenched bond-mixed spin-$\frac{1}{2}$ Ising magnet in an anisotropic simple cubic lattice. Its Hamiltonian is given by

$$\mathcal{H} = -\sum_{<i,j>} J_{ij}\sigma_i\sigma_j \qquad (\sigma_i, \sigma_j = \pm 1) \tag{1}$$

where $<i,j>$ runs over all the nearest-neighboring couples of sites of a simple cubic lattice; J_{ij} is a random variable associated with three different distribution laws respectively along the three crystalline directions (denoted by 1, 2 and 3), namely

$$P_r(J_{ij}) = (1-p_r)\delta(J_{ij}-J'_r) + p_r\delta(J_{ij}-J_r) \qquad (r=1,2,3) \tag{2}$$

where we assume $0 \leq p_r \leq 1$ $(\forall r)$, $0 \leq J_1 \leq J_2 \leq J_3 > 0$, and $J'_r \leq J_r (\forall r)$. It is important to note that these are conventional restrictions, and not physical ones.

The phase diagram of this model involves a 9-dimensional space (determined, for instance, by k_BT/J_3, J_2/J_3, J_1/J_3, J'_1/J_1, J'_2/J_2, J'_3/J_3, p_1, p_2, p_3); more specifically the critical frontier separating the paramagnetic phase from any other (corresponding,

more precisely, to the stability limit of the paramagnetic phase) consists in a 8-dimensional hypersurface in the above mentioned hyperspace. Such a complex critical frontier has obviously to be studied through its particular cases. In paper I we have presented the general formalism (which is a considerable improvement on the Mean Field Approximation (MFA); see paper I and references therein), and discussed a large number of particular cases (*anisotropic* coupling constants) restricted however to *isotropic* concentrations ($p_1 = p_2 = p_3$). In the present paper we assume *isotropic* coupling constants ($J_1 = J_2 = J_3 \equiv J$ and $J_1' = J_2' = J_3' \equiv J'$) but allow for *anisotropic* concentrations.

In Section II the formalism is briefly recalled (in a form slightly more convenient than that introduced in paper I), and in Section III the most interesting particular phase diagrams are presented and discussed. Finally we conclude in Section IV.

II. FORMALISM

The system determined by Eqs. (1) and (2) can be treated by using the following Callen identity[2]:

$$\langle \sigma_i \rangle = \langle \tanh \beta \sum_j J_{ij} \sigma_j \rangle \qquad (3)$$

where $\beta \equiv 1/k_B T$, $\langle \cdots \rangle$ indicates the canonical thermal average associated with a fixed configuration of $\{J_{ij}\}$, and the sum runs over all the sites to which site i is connected (in the

present case, first-neighboring ones). This identity can be re written[3], by introducing the differential operator $D \equiv \partial/\partial x$, as follows

$$\langle \sigma_i \rangle = \langle \exp(\beta D \sum_j J_{ij}\sigma_j) \rangle \tanh x \Big|_{x=0}$$

$$= \langle \prod_j [\cosh(\beta D J_{ij}) + \sigma_j \sinh(\beta D J_{ij})] \rangle \tanh x \Big|_{x=0} \qquad (4)$$

Now we apply on both sides of this equation the configurational average (denoted by $\langle \cdots \rangle_J$), and obtain

$$m \equiv \langle\langle \sigma_i \rangle\rangle_J = \langle\langle \prod_j [\cosh(\beta D J_{ij}) + \sigma_j \sinh(\beta D J_{ij})] \rangle\rangle_J \tanh x \Big|_{x=0} \qquad (5)$$

It is worthy to note that this is still an exact relation. By assuming now the same decouplings of paper I (essentially, neglecting multispin correlations), Eq. (5) yields

$$m = \prod_{r=1}^{3} \{ [(1-p_r)(\cosh(\beta D J'_r) + m \sinh(\beta D J'_r))$$

$$+ p_r (\cosh(\beta D J_r) + m \sinh(\beta D J_r))]^2 \} \tanh x \Big|_{x=0} \qquad (6)$$

Along the last step we have lost the strict criticality of the system (e.g., the critical exponents are going to be classical ones, and the real dimensionality of the system will be taken into account only through the coordination number); however, the present effective-field theory is quite superior to the MFA one, as extensively exhibited in paper I and references therein.

A tedious but straightforward evaluation of Eq.(6) leads to

$$m = 2Am + 2Bm^3 + 2Cm^5 \tag{7}$$

where the coefficients A, B and C are functions of $(k_BT/J_3, J_2/J_3, \ldots, p_1, p_2, p_3)$; they are indicated in the Appendix for the particular case $J_1 = J_2 = J_3 \equiv J$ and $J'_1 = J'_2 = J'_3 \equiv J'$, in which we are presently interested. Eq.(7) admits two solutions, namely $m \equiv 0$ (paramagnetic phase) and

$$m = \left\{\frac{-B-[B^2-2C(2A-1)]^{1/2}}{2C}\right\}^{1/2} \tag{8}$$

(ferromagnetic phase). The critical hypersurface characterizing the ferromagnetic-phase stability limit is determined by

$$A = 1/2 \tag{9}$$

In what follows we discuss the phase diagrams corresponding to the main particular cases not covered in paper I.

III. PARTICULAR CASES

Herein we present the phase diagrams associated with the isotropic coupling constant models ($J_r \equiv J$ and $J'_r \equiv J'$ for $r = 1,2,3$).

A. Bond-diluted (J'=0) and bond-mixed (J'/J>0) models

The coefficient A appearing in Eq.(9) is given by the t'=0 particular case of Eq.(A.1). At vanishing temperature (T=0), the critical surface is given by

$$\frac{15}{16}(p_1p_2p_3)^2 + (1-p_1)(1-p_2)(1-p_3)\,\alpha(p_1,p_2,p_3) + \frac{15}{8}\,p_1p_2p_3\alpha(1-p_1,1-p_2,1-p_3)$$

$$+ \frac{1}{2}[\alpha(p_1,p_2,p_3)]^2 + (1-p_1)(1-p_2)(1-p_3)\alpha(1-p_1,1-p_2,1-p_3)$$

$$+ \frac{3}{4}[\alpha(1-p_1,1-p_2,1-p_3)]^2 + \frac{3}{2}\,p_1p_2p_3\alpha(p_1,p_2,p_3)$$

$$+ \frac{3}{2}\alpha(p_1,p_2,p_3)\alpha(1-p_1,1-p_2,1-p_3)$$

$$+ \frac{3}{2}p_1p_2p_3(1-p_1)(1-p_2)(1-p_3) = \frac{1}{2} \qquad (10)$$

where α is defined by Eq.(A.8).

This equation provides the results indicated in Fig. 1. The two- and three-dimensional isotropic percolation thresholds respectively are 0.4284 (to be compared with the exact result[4] $p_c = 1/2$ and the MFA result $p_c = 0$), and 0.2929 (to be compared with the series result[5] $p_c \simeq 0.247$ and the MFA result $p_c = 0$).

The type of equation appearing for the finite temperature critical surface can be illustrated through the $p_2 = 0$ particular case:

$$(1-p_1)(1-p_3)[p_1(1-p_3)+p_3(1-p_1)]\tanh t$$

$$+\frac{1}{2}\{[p_1(1-p_3)+p_3(1-p_1)]^2+2p_1p_3(1-p_1)(1-p_3)\}\tanh(2t)$$

$$+\frac{1}{4}p_1^2p_3^2[\tanh(4t)+2\tanh(2t)]$$

$$+\frac{3}{4}\{p_1p_3[p_1(1-p_3)+p_3(1-p_1)][\tanh(3t)+\tanh t]\}=\frac{1}{2} \qquad (11)$$

Typical results are indicated in Figs. 2-4. The two-and three-dimensional critical points respectively are $k_BT_c/J \simeq 3.0898$ (to be compared with the exact result 2.2692, and the MFA result 4), and $k_BT_c \simeq 5.0733$ (to be compared with the series result[6] 4.5112, and the MFA result 6).

B. Competing interactions bond-mixed models ($J'/J < 0$)

Consider now the case where the interactions are competing (typically $J > 0$ and $J' < 0$). New physical situations appear in the sense that the critical temperature vanishes now at concentrations (of J) *higher* than the percolation threshold(the higher the more negative J'/J is). Typical results are indicated in Fig. 5 and 6. The two- and three-dimensional critical concentrations associated with the isotropic $J'/J = -1$ model respectively are $p_c = 5/6 \simeq 0.833$ (to be compared with the values 0.8-0.85 by Monte Carlo[7], 0.834 by the replica method[8], 0.833 by the Bethe method[9]) and $p_c = 23/30 \simeq 0.767$.

IV. CONCLUSION

We have discussed the quenched bond-mixed first-neighboring spin $-\frac{1}{2}$ Ising model (with both competing and non-competing interactions) on an anisotropic cubic lattice. An analytic explicit expression for the spontaneous magnetization has been obtained within an effective field framework which is based on the introduction of a convenient differential operator [3] in the Callen identity[2]. This approximation has been analyzed in detail in paper I [1]. We have herein focused the case where the anisotropy in the cubic lattice comes from the various *concentrations* of the interactions (in contrast with paper I where the source of anisotropy was the various *interactions*). The phase diagrams (stability limit of the ferromagnetic phase) corresponding to various typical cases have been exhibited (see Figs. 1-7). Several non trivial "crossings" and non-uniform convergences effects have been illustrated. Whenever comparison with other available results was possible, the agreement has been qualitatively (and to a certain extent quantitatively) quite satisfactory. The picture which emerges gives an overall view of the richness of situations that could occur in the phase diagrams of real substances.

This work has been partially supported by CNPq and FINEP (Brazil).

Appendix

The coefficients A, B and C appearing in Eqs.(7) and (8) are given by

$$A = \sum_{i=1}^{4} [a_i(p_1,p_2,p_3) f_i(t,t') + a_i(1-p_1,1-p_2,1-p_3) f_i(t',t)] \tag{A.1}$$

$$B = \sum_{i=1}^{4} [b_i(p_1,p_2,p_3) g_i(t,t') + b_i(1-p_1,1-p_2,1-p_3) g_i(t',t)] \tag{A.2}$$

$$C = \sum_{i=1}^{4} [a_i(p_1,p_2,p_3) h_i(t,t') + a_i(1-p_1,1-p_2,1-p_3) h_i(t',t)] \tag{A.3}$$

where

$$a_i(p_1,p_2,p_3) = \frac{3}{10} b_1(p_1,p_2,p_3) = 3(p_1p_2p_3)^2 \tag{A.4}$$

$$a_2(p_1,p_2,p_3) = \frac{1}{10} b_2(p_1,p_2,p_3) = (1-p_1)(1-p_2)(1-p_3)\,\alpha(p_1,p_2,p_3) \tag{A.5}$$

$$a_3(p_1,p_2,p_3) = \frac{1}{2} b_3(p_1,p_2,p_3) =$$

$$= [\alpha(p_1,p_2,p_3)]^2 + 2(1-p_1)(1-p_2)(1-p_3)\,\alpha(1-p_1,1-p_2,1-p_3) \tag{A.6}$$

$$a_4(p_1,p_2,p_3) = 3b_4(p_1,p_2,p_3) =$$

$$= 3[\alpha(p_1,p_2,p_3)\alpha(1-p_1,1-p_2,1-p_3) + p_1p_2p_3(1-p_1)(1-p_2)(1-p_3)] \tag{A.7}$$

with

$$\alpha(p_1,p_2,p_3) = p_1(1-p_2)(1-p_3) + (1-p_1)p_2(1-p_3) + (1-p_1)(1-p_2)p_3 \tag{A.8}$$

and where

$$f_1(t,t') = \frac{1}{32}[\tanh(6t) + 4\tanh(4t) + 5\tanh(2t)] \tag{A.9}$$

$$f_2(t,t') = \frac{1}{32}[6\tanh(5t'+t) + 20\tanh(3t'+t) + 20\tanh(t'+t) + 10\tanh(3t'-t) + 4\tanh(5t'-t)] \tag{A.10}$$

$$f_3(t,t') = \frac{1}{32}[3\tanh(4t'+2t) + 8\tanh(2t'+2t) + 6\tanh(2t) + \tanh(4t'-2t) + 4\tanh(4t') + 8\tanh(2t')] \tag{A.11}$$

$$f_4(t,t') = \frac{1}{32}[\tanh(3t'+3t) + 3\tanh(t'+3t) + 3\tanh(3t-t') + \tanh(3t-3t') + \tanh(3t'+t) + 3\tanh(t'+t) + 3\tanh(t-t') + \tanh(t-3t')] \tag{A.12}$$

$$g_1(t,t') = \frac{1}{32}[\tanh(6t) - 3\tanh(2t)] \tag{A.13}$$

$$g_2(t,t') = \frac{1}{32}[2\tanh(5t'+t) - 4\tanh(t'+t) + 2\tanh(t'-3t)] \tag{A.14}$$

$$g_3(t,t') = \frac{1}{32}[5\tanh(4t'+2t) + \tanh(2t-4t') - 8\tanh(2t') - 6\tanh(2t)] \quad (A.15)$$

$$g_4(t,t') = \frac{1}{32}[10\tanh(3t+3t') - 12\tanh(3t+t') + 6\tanh(t'-3t) + 8\tanh(3t-3t') + 12\tanh(t+3t') - 18\tanh(t+t') + 6\tanh(t-3t')] \quad (A.16)$$

$$h_1(t,t') = \frac{1}{32}[\tanh(6t) - 4\tanh(4t) + 5\tanh(2t)] \quad (A.17)$$

$$h_2(t,t') = \frac{1}{32}[6\tanh(5t'+t) - 20\tanh(3t'+t) + 20\tanh(t'+t) + 10\tanh(3t'-t) + 4\tanh(t-5t')] \quad (A.18)$$

$$h_3(t,t') = \frac{1}{32}[3\tanh(4t'+2t) - 8\tanh(2t'+2t) + 6\tanh(2t) + \tanh(4t'-2t) - 4\tanh(4t') + 8\tanh(2t')] \quad (A.19)$$

$$h_4(t,t') = \frac{1}{32}[\tanh(3t'+3t) - 3\tanh(t'+3t) + 3\tanh(3t-t') + \tanh(3t'-3t) - \tanh(3t'+t) + 3\tanh(t'+t) + 3\tanh(t'-t) + \tanh(t-3t')] \quad (A.20)$$

with $t \equiv J/k_BT$ and $t' \equiv J'/k_BT = (J'/J)t$.

REFERENCES

[1] E.F. Sarmento and C. Tsallis, Phys. Rev. B 27, 5784 (1983).

[2] H.B. Callen, Phys. Lett. 4, 161 (1963).

[3] R. Honmura and T. Kaneyoshi, Prog. Theor. Phys. 60, 635 (1978); J. Phys. C 12, 3979 (1979).

[4] M.F. Sykes and J. Essam, Phys. Rev. Lett. 10, 3 (1963).

[5] D.S. Gaunt and H. Ruskin, J. Phys. A 11, 1369 (1978).

[6] J. Zinn-Justin, J. Phys. (Paris) 40, 969 (1979).

[7] S. Kirkpatrick, Phys. Rev. B 15, 1533 (1977).

[8] E. Domany, J. Phys. C 12, L 119 (1979).

[9] S. Katsura, S. Inawashiro and S. Fujiki, Physica A 99, 193 (1979).

CAPTION FOR FIGURES

Fig. 1 - T=0 phase diagram of the bond-dilute (J'=0) ferromagnet. (a) percolation critical surface (indicative); (b) fixed p_3 and (c) fixed p_2/p_1 cross-sections.

Fig. 2 - Phase diagram of the d=2 (p_2=0) bond-dilute (J'=0) ferromagnet. (a) fixed p_3 and (b) fixed $(1-p_3)/(1-p_1)$ cross-sections.

Fig. 3 - Phase diagram of the d=3 bond-dilute (J'=0) ferromagnet: typical cross-sections. (a) $p_1 = p_3$; (b) $p_1 = p_3$ and fixed p_2/p_1; (c) $p_1=p_2$ and fixed $(1-p_3)/(1-p_1)$ (values indicated on the curves); (d) p_3=1.

Fig. 4 - Phase diagram of the d=3 bond-mixed non-competing interactions ($J'/J \geq 0$) ferromagnet: typical cross-sections. (a) $J'/J=0.5$, $p_2/p_1=0.5$ and $p_3/p_1=1$; (b) $J'/J=0.1$, $p_2/p_1=0.5$ and $p_3/p_1=1$; (c) $J'/J=0.01$, $p_2/p_1=0.5$ and $p_3/p_1=1$; (d) $J'/J=0$, $p_2/p_1=0.5$ and $p_3/p_1=1$; (e) $J'/J=0.01$, $p_2/p_1=0.1$ and $p_3/p_1=1$; (f) $J'/J=0.01$, $p_2/p_1=0.5$ and $p_3/p_1=0$; (g) $J'/J=0.01$, $p_2/p_1=0.1$ and $p_3/p_1=0.01$.

Fig. 5 - T=0 phase diagram of the d=3 bond-mixed competing interactions ($J'/J<0$) ferromagnet: typical cross-sections. (a) fixed p_1 (indicated on curves); (b) fixed p_2/p_1; (c) fixed p_2/p_1.

Fig. 6 - Phase diagram of the d=3 bond-mixed competing interactions ($J'/J<0$) ferromagnet: typical cross-sections. (a) $p_2=p_1$ and fixed $(1-p_3)/(1-p_1)$. (b) various situations: $p_1=p_2=p_3$ (curve a); $p_2/p_1=0.5$ and $(1-p_3)/(1-p_1)=0.1$

(curve b); $p_2/p_1=0.5$ and $(1-p_3)/(1-p_1)=1$ (curve c); $(1-p_2)/(1-p_1)=0.1$ and $p_3=0$ (curve d); $(1-p_2)/(1-p_1)=1$ and $p_3=0$ (curve e).

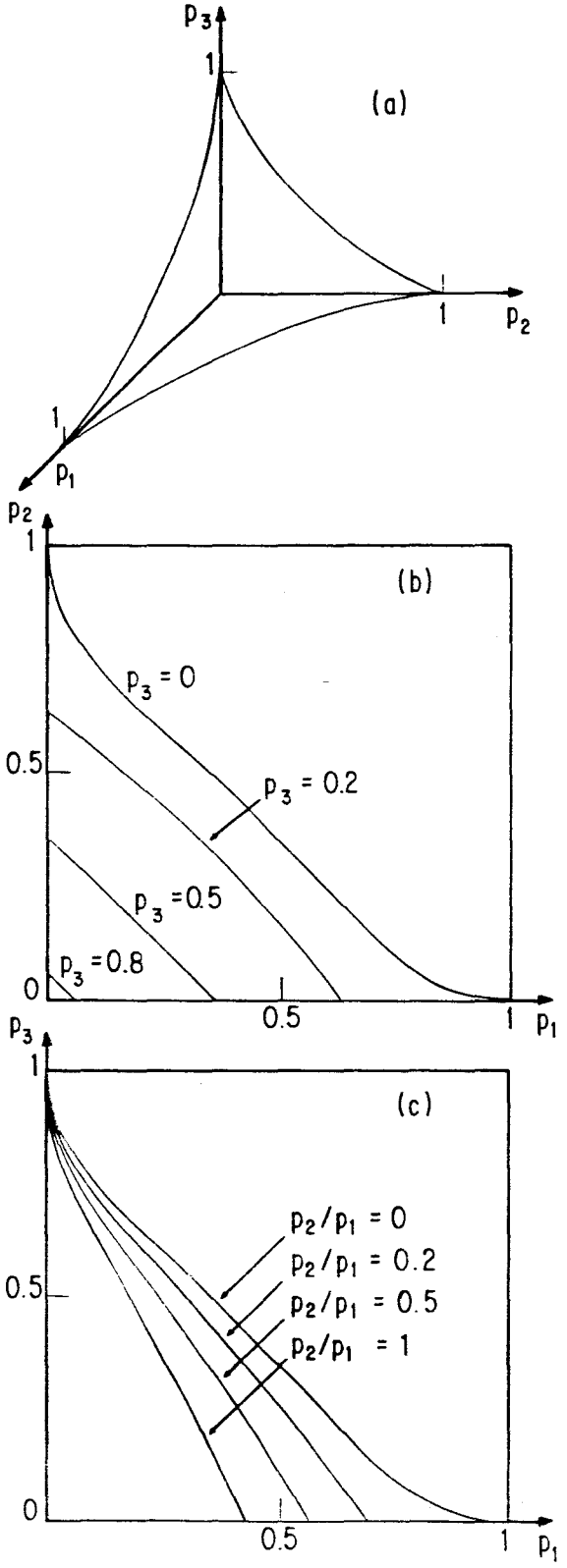
p3
1
(a)
1
p2
1
p1
p2
1
(b)
p3 = 0
0.5
p3 = 0.2
p3 =0.5
p3 =0.8
0
0.5
1
p1
p3
1
(c)
p2/p1 = 0
p2/p1 = 0.2
0.5
p2/p1 = 0.5
p2/p1 = 1
0
0.5
1
p1

FIG.1

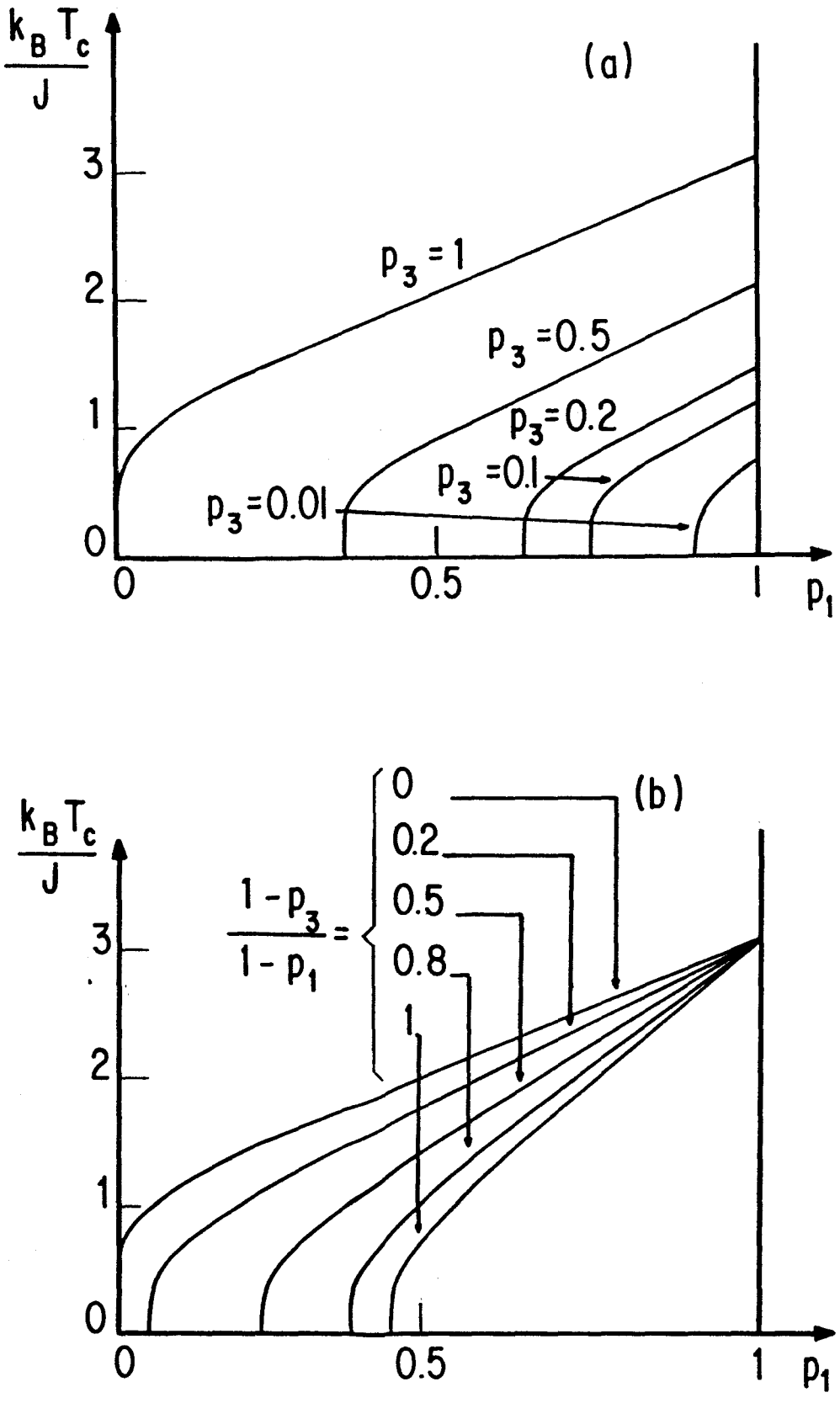
$\frac{k_B T_c}{J}$
(a)
3
2
1
0
$p_3 = 1$
$p_3 = 0.5$
$p_3 = 0.2$
$p_3 = 0.1$
$p_3 = 0.01$
0
0.5
1
p_1
$\frac{k_B T_c}{J}$
$\frac{1-p_3}{1-p_1} =$
0
0.2
0.5
0.8
1
(b)
3
2
1
0
0
0.5
1
p_1

FIG. 2

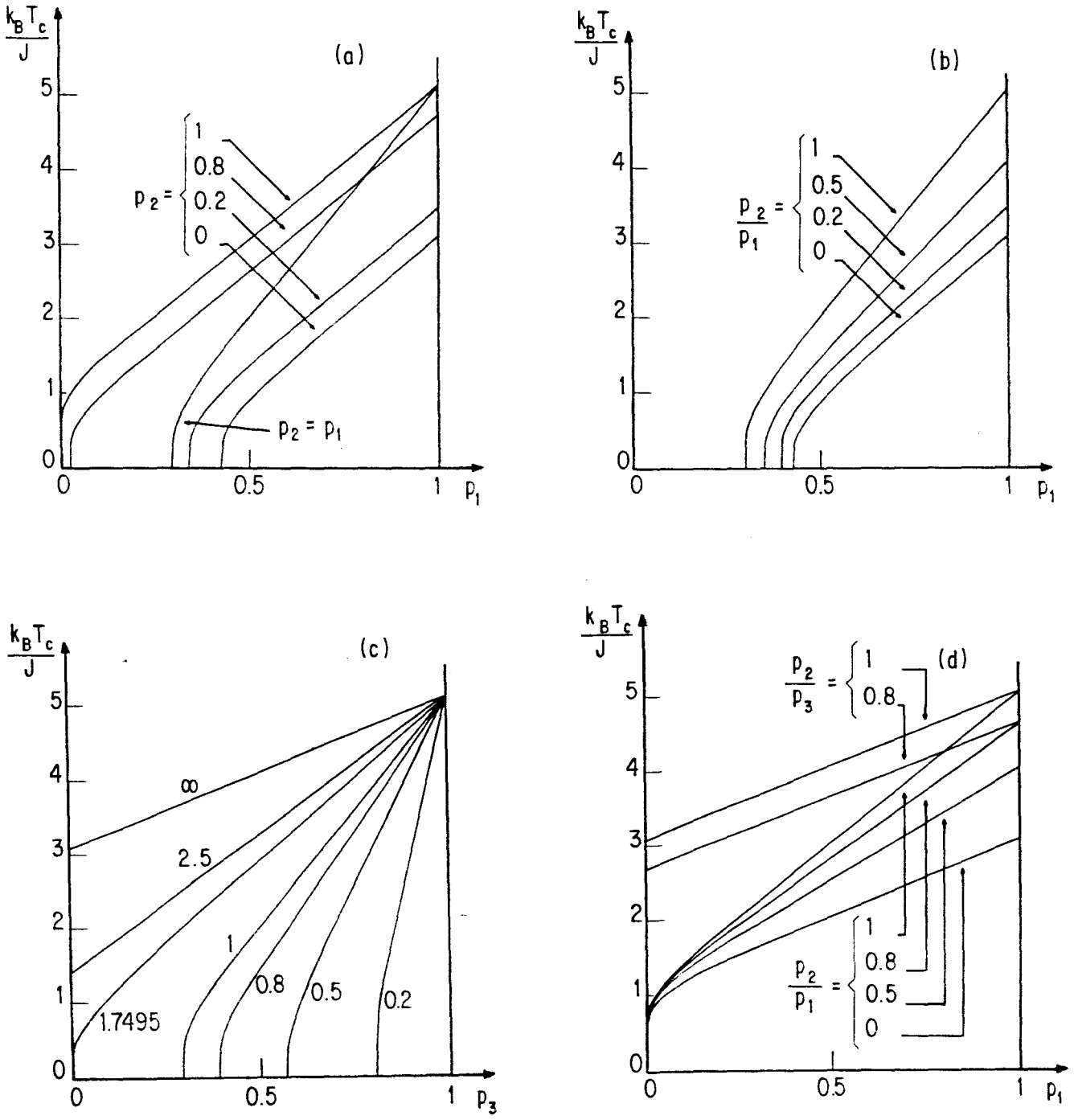
(a)
$\frac{k_B T_c}{J}$
$p_2 =$ 1, 0.8, 0.2, 0
$p_2 = p_1$
p_1
(b)
$\frac{p_2}{p_1} =$ 1, 0.5, 0.2, 0
p_1
(c)
$\frac{k_B T_c}{J}$
∞, 2.5, 1, 0.8, 0.5, 0.2, 1.7495
p_3
(d)
$\frac{p_2}{p_3} =$ 1, 0.8
$\frac{p_2}{p_1} =$ 1, 0.8, 0.5, 0
p_1

FIG. 3

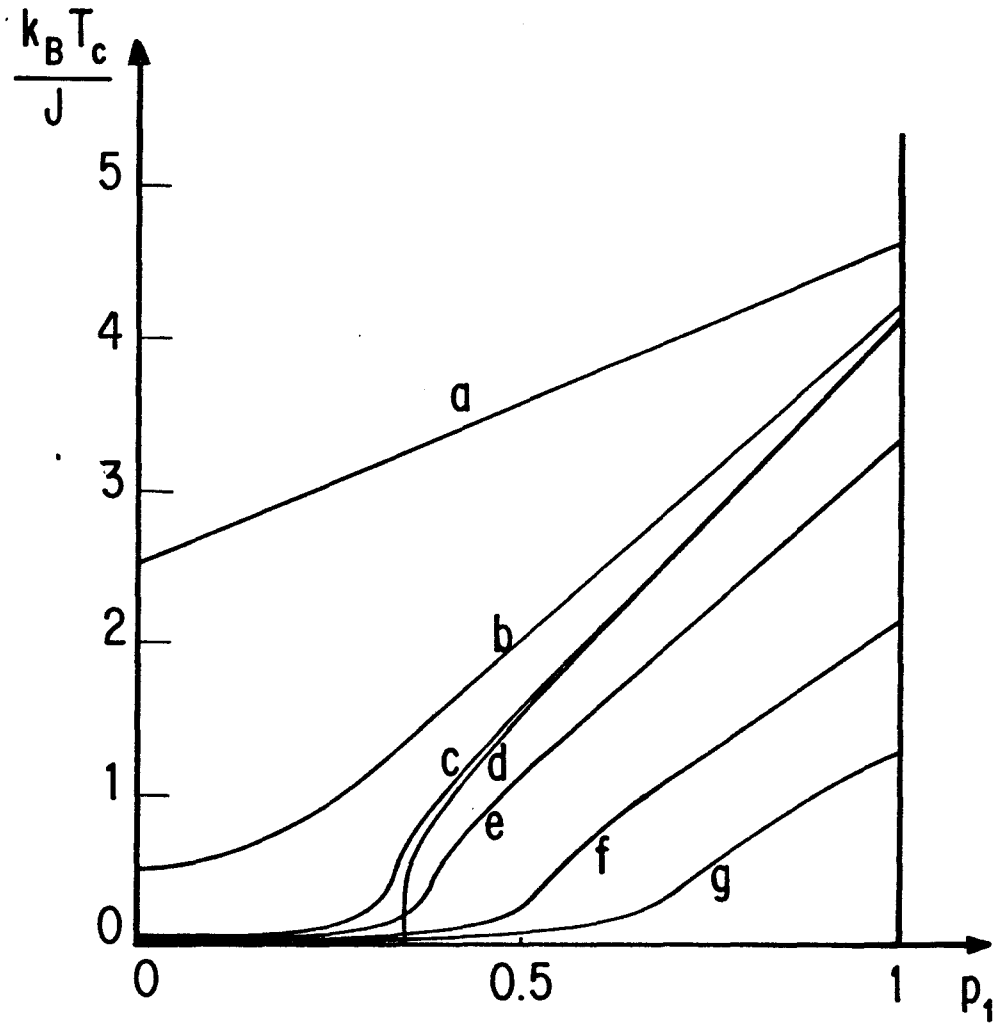

FIG.4

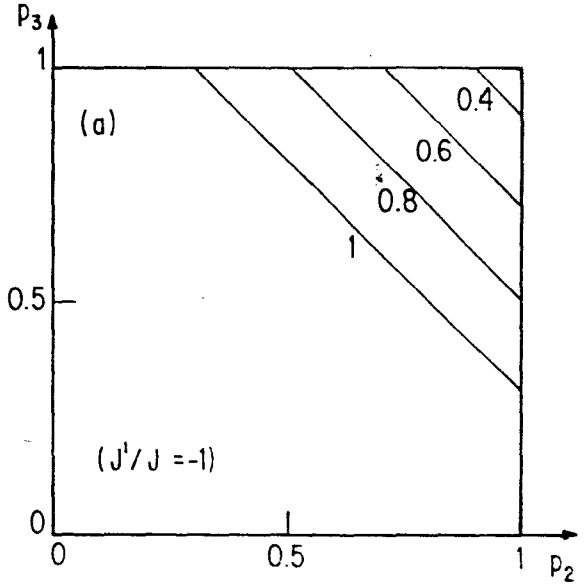
p_3
1
0.5
0
(a)
0.4
0.6
0.8
1
$(J'/J = -1)$
0
0.5
1
p_2

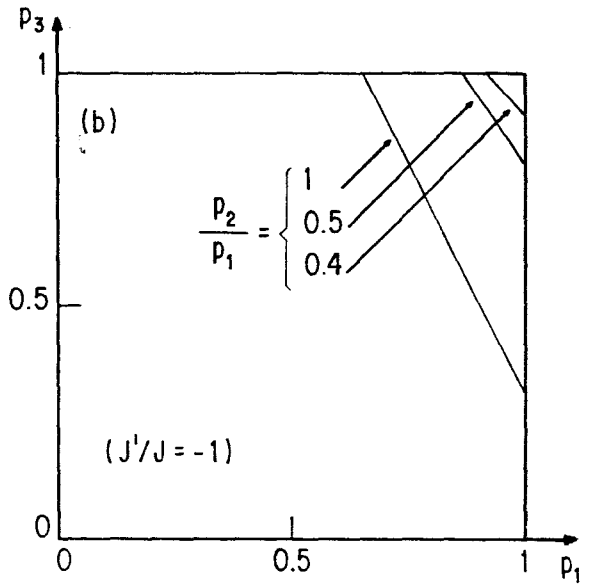
p_3
1
0.5
0
(b)
$\frac{p_2}{p_1} = \begin{cases} 1 \\ 0.5 \\ 0.4 \end{cases}$
$(J'/J = -1)$
0
0.5
1
p_1

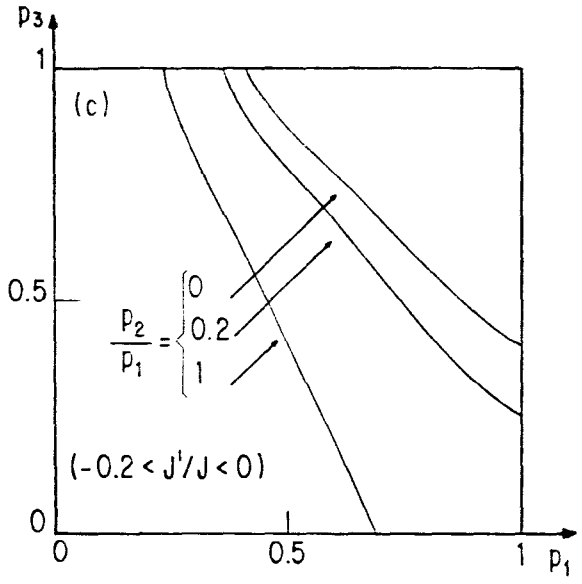
p_3
1
0.5
0
(c)
$\frac{p_2}{p_1} = \begin{cases} 0 \\ 0.2 \\ 1 \end{cases}$
$(-0.2 < J'/J < 0)$
0
0.5
1
p_1

FIG. 5

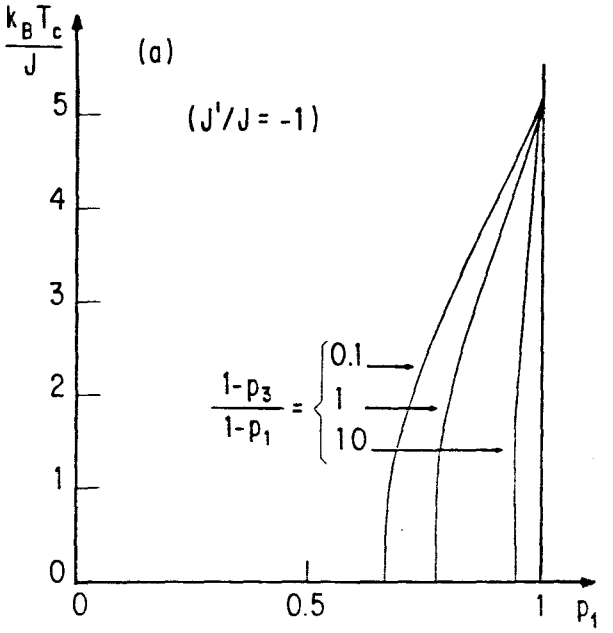
$\frac{k_B T_c}{J}$
(a)
$(J'/J = -1)$
5
4
3
2
1
0
$\frac{1-p_3}{1-p_1} = \begin{cases} 0.1 \\ 1 \\ 10 \end{cases}$
0
0.5
1
p_1

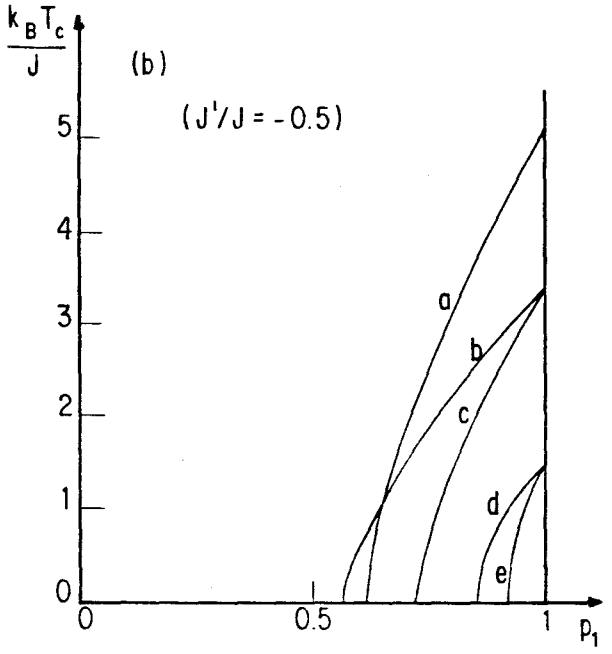
$\frac{k_B T_c}{J}$
(b)
$(J'/J = -0.5)$
5
4
3
2
1
0
a
b
c
d
e
0
0.5
1
p_1

FIG. 6